Short Communication

Highly efficient V–Sb–O/SiO$_2$ catalyst with Sb atom-isolated VOx species for oxidative dehydrogenation of propane to propene

Haidong Zhang [a,*], Shujie Cao [a], Yu Zou [a], Yi-Meng Wang [b,**], Xiaojing Zhou [c], Yu Shen [a], Xuxu Zheng [a]

[a] Key laboratory of Catalysis Science and Technology of Chongqing Education Commission, Chongqing Technology and Business University, Chongqing 400067, China
[b] Shanghai Key Lab of Green Chemistry and Chemical Processes, Department of Chemistry, East China Normal University, Shanghai 200062, China
[c] Centre for Organic Electronics, School of Mathematical and Physical Sciences, Faculty of Science and IT, University of Newcastle, Callaghan, NSW 2308, Australia

ARTICLE INFO

ABSTRACT

Silica supported vanadium–antimony mixed oxide catalyst (V–Sb–O/SiO$_2$) with the $-O-Sb-O-V-O-Sb-$ framework was prepared by a two-step impregnation method, in which SbCl$_5$ and NH$_4$VO$_3$ were introduced successively to generate monomeric VOx species isolated by Sb atoms. In the ODH of propane with O$_2$ as oxidant, the V–Sb–O/SiO$_2$ catalyst leads to high activity and high propene selectivity but depressed production of COx. At 600 °C, a 65.6% C$_3$H$_6$ selectivity with a 40.1% C$_3$H$_8$ conversion was obtained and then, a propene yield up to 26.3% was achieved on V–Sb–O/SiO$_2$ catalyst. This yield is comparable to that for V–Mg–O catalysts, SBA-15/MCM-41supported vanadia catalysts and vanadium-containing mesoporous silica materials.

© 2013 Elsevier B.V. All rights reserved.

1. Introduction

Propene is one of the most important chemicals and widely used for the production of many different polymers and chemical intermediates [1]. The oxidative dehydrogenation (ODH) of propane to produce propene is a very promising process to obtain propene in comparison to the processes with oil as feedstock [2,3]. A desirable catalyst for the ODH of propane must be able to effectively activate the C–H bond of propane and hinder undesirable deep oxidation of propene to COx [4]. Supported vanadia catalysts have been found to be highly desirable for this reaction [2,4–7]. It has been generally agreed that highly isolated VOx species are active sites for the selective formation of propene but polymeric and crystalline VOx species are those responsible for the deep oxidation of propene to COx [2,5,7].

The support materials with high specific area, e.g., MCM-41 and SBA-15, were widely used to prepared supported vanadia catalysts with highly isolated VOx species because they are predominantly formed at low vanadium density [5,8,9]. However, the aggregation of highly isolated VOx species to generate crystalline V$_2$O$_5$ cannot be avoided under reaction condition even the surface vanadium density is as low as 2.0–3.1 V·nm^{-2} [2,10,11]. Vanadium-containing mesoporous silica materials have also been developed in order to obtain highly isolated VOx species [12–17]. Unfortunately, the big difference between vanadium atoms and silica framework leads to the problems

like low vanadium content in silica framework, leaching of vanadium atoms and decreased stability of vanadium-containing silica framework, which are still open issues in this field [18,19].

One of the most beautiful and lucid examples of site isolation is USb$_3$O$_{10}$ catalyst, in which U atoms are completely isolated from each other by Sb atoms [20]. In vanadium–antimony mixed, VOx species can also be interrupted by the incorporation of Sb atoms and thus monomeric VOx species can be obtained [21]. This provides a potentially promising route to achieve highly isolated VOx species. Herein, we report the speciation of Sb atom isolated VOx species on V–Sb–O/SiO$_2$ catalyst and its high efficiency in the oxidative dehydrogenation of propane to propene using O$_2$ as oxidant.

2. Experimental

V–Sb–O/SiO$_2$ catalyst was prepared using an incipient wetness impregnation method with two steps. Silica was firstly impregnated with SbCl$_5$–absolute ethanol solution, and then dried at room temperature. This impregnated silica was then impregnated for the second time with aqueous solution of NH$_4$VO$_3$ and then dried at room temperature. The pH value of the final impregnated silica was adjusted to 8 using aqueous ammonia solution and then dried at 100 °C and calcined at 700 °C for 4 h with the supply of air to obtain V–Sb–O/SiO$_2$ catalyst. VOx/SiO$_2$ and SbOx/SiO$_2$ catalysts were prepared by the incipient wetness impregnation of silica with aqueous solution of NH$_4$VO$_3$ and SbCl$_5$–ethanol solution, respectively. The procedures for the adjustment of pH value, drying and calcination of SbOx/SiO$_2$ catalyst or VOx/SiO$_2$ catalysts were same as that of V–Sb–O/SiO$_2$ catalyst. The characterizations of all catalysts are described in Supplementary information in

* Corresponding author.
** Corresponding author. Tel./fax: +86 23 62768317, +86 21 62232251.
E-mail addresses: haidongzhang@ctbu.edu.cn (H. Zhang), ymwang@chem.ecnu.edu.cn (Y.-M. Wang).

details. The texture properties and V/Sb loadings of all catalysts are shown in Table 1 and Figs. S1–4.

The ODH reaction tests were performed in a quartz tubular reactor at atmospheric pressure using O_2 as oxidant. The feeding mixture of $C_3H_8/O_2/N_2$ had a molar ratio of 1/1/8. In each test, 0.1 g catalyst was used and the flow rate of feeding mixture was 0.134 mol (STY) h^{-1}. A SHIMADZU GC 2010 gas chromatograph, which was equipped by a FID detector connected to a Porapak Q column and a TCD detector connected to a TDX-01 column, was used to do on-line analysis of products. The conversion of propane and propene selectivity was calculated as the following equations [1]:

$$Conversion = (M_{in}\text{-}M_{out})/M_{in} \times 100\%$$

$$C_3H_6 \ Selectivity = n(C_3H_6)/(M_{in}\text{-}M_{out}) \times 100\%$$

$$C_3H_6 \ Yield = C_3H_6 \ Selectivity \times Conversion$$

where M_{in} and M_{out} are the amounts (mole) of propane introduced in and remaining in effluent, respectively. $n(C_3H_6)$ is the amount (mole) of propene detected in effluent. It was observed that $SbOx/SiO_2$ catalyst was much less active than either VOx/SiO_2 or V–Sb–O/SiO$_2$ catalyst.

3. Results and discussion

Fig. 1 shows the XRD patterns of silica support, SbOx/SiO$_2$, VOx/SiO$_2$ and V–Sb–O/SiO$_2$ catalysts. The XRD pattern of SiO$_2$ only exhibits a broad peak (halo, 2 theta = 15–30°) attributed to amorphous silica. The pattern of SbOx/SiO$_2$ catalyst also only shows this amorphous halo, being coincident with the highly dispersion of antimony oxide on silica [22]. Additionally, the XRD pattern of SbOx/SiO$_2$ catalyst demonstrates no diffraction peak of crystalline antimony oxide even its loading reaches 20 wt.% [23,24]. The pattern of VOx/SiO$_2$ catalyst shows very small but identified diffraction peaks at 20.5°, 26.4°, 31.2°, 47.3° and 51.1°, reflecting the formation of crystalline vanadium oxides. In the pattern of V–Sb–O/SiO$_2$, the diffraction peaks at 27.4°, 30.6°, 31.5°, 33.9°, 35.3°, 37.2°, 41.3°, 48.4°, 50.3°, 53.5° and 53.8° can be ascribed to the characteristic diffraction peaks of antimony–vanadium mixed oxides in the phases of Sb$_2$VO$_5$ and SbVO$_4$/VSb$_{1-x}$O$_{4-1.5x}$ [21,25].

Fig. 2 gives the H$_2$-TPR profiles of SbOx/SiO$_2$, VOx/SiO$_2$ and V–Sb–O/SiO$_2$ catalysts. The TPR profile of VOx/SiO$_2$ catalyst shows a reduction peak at 542 °C, attributed to the reduction of highly isolated tetrahedral or low oligomeric V^{5+} entities [12]. The TPR profile of SbOx/SiO$_2$ catalyst gives a very broad reduction band arising at 320 °C and reaching a maximum at 800 °C. Being much different to the profiles of SbOx/SiO$_2$ and VOx/SiO$_2$ catalysts, The TPR profile of V–Sb–O/SiO$_2$ catalyst gives reduction peaks in the range from 610 °C to 720 °C, suggesting the formation of antimony–vanadium mixed oxide [21].

Fig. 3 shows the UV–Vis DRS spectra of silica support, SbOx/SiO$_2$, VOx/SiO$_2$ and V–Sb–O/SiO$_2$ catalysts. No band can be identified in the spectrum of SiO$_2$. A broad band centered at 235 nm can be identified in the spectrum of SbOx/SiO$_2$. In the spectrum of VOx/SiO$_2$ catalyst, the O → V charge transfer (CT) bands centered at 257 nm and 336 nm can be identified and attributed to highly isolated monomeric VOx species and low oligomeric VOx species with V–O–V bridges,
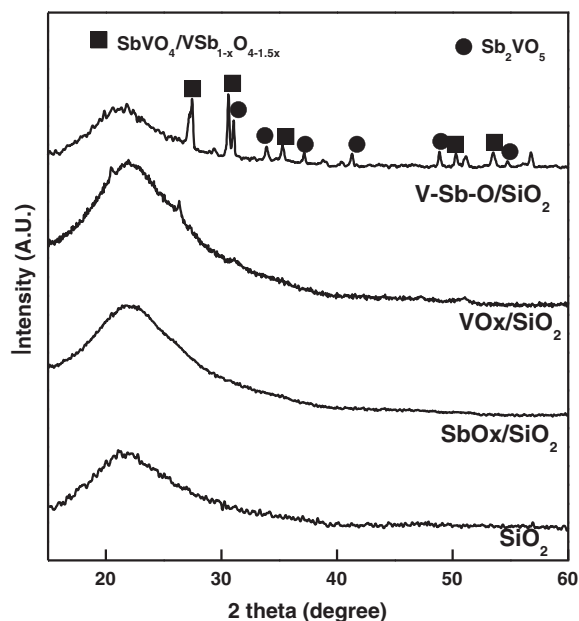

Fig. 1. XRD patterns of silica support, SbOx/SiO$_2$, VOx/SiO$_2$ and V–Sb–O/SiO$_2$ catalysts.

respectively [5,8,12,21,26]. This is consistent with the H$_2$-TPR tests of VOx/SiO$_2$ catalyst. Additionally, a broad band at 488 nm can also be discovered in the spectrum of VOx/SiO$_2$ catalyst. This indicates the formation of micro-crystalline of V$_2$O$_5$ [5,21,26], being consistent with the XRD pattern in Fig. 1. In the spectrum of V–Sb–O/SiO$_2$ catalyst, two bands centered at 244 nm and 378 nm can be observed in the shorter wavelength zone comparing with that of those bands for VOx/SiO$_2$ catalyst. The attribution of these two bands to CT bands of vanadium-containing species goes straight [21]. The band at 244 nm is related to highly isolated monomeric VOx species but located on the higher absorption energy than that of monomeric VOx species in VOx/SiO$_2$ catalyst. The reason for this phenomenon lies in two aspects. The first one is that the monomeric VOx species in V–Sb–O/SiO$_2$ catalyst are interrupted by Sb atoms and stabilized by V–O–Sb bridges [21].
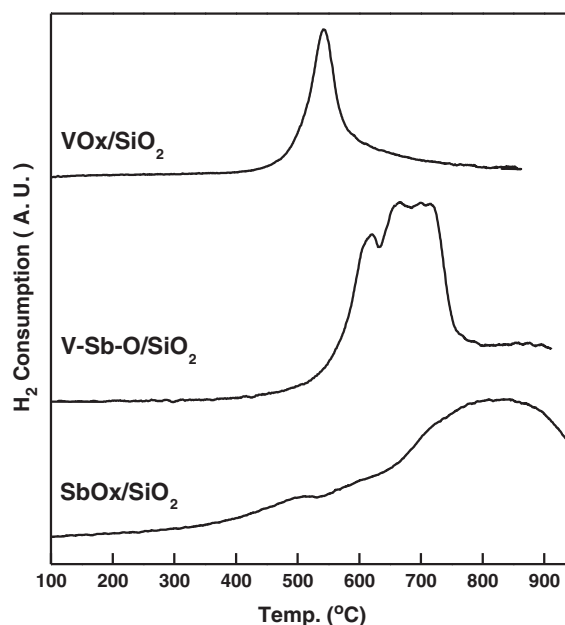
Table 1
Textural properties and V/Sb loading of SiO$_2$, V–Sb–O/SiO$_2$, VOx/SiO$_2$ and SbOx/SiO$_2$ catalysts.

Catalysts	Specific area (m^2/g)	Average pore size (nm)	Loading of Sb or V	Sb/V molecular ratio
SiO$_2$	420	8.8	–	–
SbOx/SiO$_2$	360	8.2	19.0 wt.% in Sb$_2$O$_5$	–
VOx/SiO$_2$	405	8.6	5.8 wt.% in V$_2$O$_5$	–
V–Sb–O/SiO$_2$	325	5.9	19.8 wt.% in Sb$_2$O$_5$ 5.7 wt.% in V$_2$O$_5$	1.94

Fig. 2. H$_2$-TPR profiles of SbOx/SiO$_2$, VOx/SiO$_2$ and V–Sb–O/SiO$_2$ catalysts.
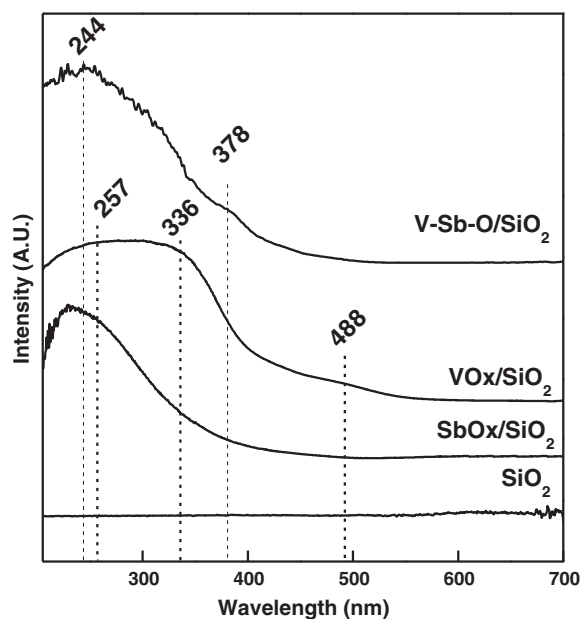
Fig. 3. UV–Vis DRS spectra of silica support, SbO_x/SiO_2, VO_x/SiO_2 and V–Sb–O/SiO_2 catalysts.

The second one is that the V–O–Sb bridges show a higher energy absorption edge than V–O–V bridges in VO_x/SiO_2 catalyst due to different electronegativities of Sb and V [21,27]. Consequently, the band at 378 nm should be attributed to V–O–Sb bridges.

The Raman spectra shown in Fig. 4 give more information about the vanadia species on VO_x/SiO_2 and V–Sb–O/SiO_2 catalysts. In the spectrum of V–Sb–O/SiO_2 catalyst, two bands at 901 and 1026 cm^{-1} can be identified and attributed to the V–O–Sb stretching mode and the V=O stretching vibration mode of vanadium–antimony mixed oxide, respectively, with another band centered at 395 cm^{-1} related to Sb_2O_4 can also be observed [21,27–30]. This reflects the formation of vanadium–antimony mixed oxide domains with V=O sites exposed. In the spectrum of VO_x/SiO_2 catalyst, the bands at 1026 and 873 cm^{-1} related to monomeric VO_x species and polymeric $(VO_3)n$ species can be observed as
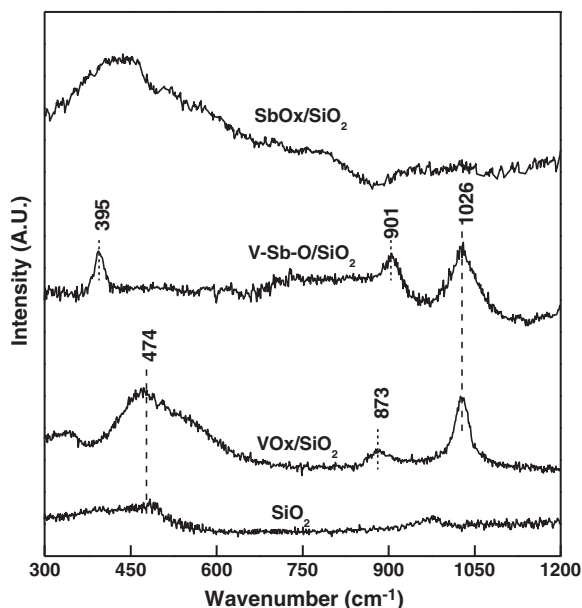
well as the band at ca. 474 cm^{-1} for amorphous silica [27,29,31]. In line with the UV–Vis DRS spectra, we can know that the amount of aggregated VO_x species in VO_x/SiO_2 catalyst is remarkably higher than that in V–Sb–O/SiO_2 catalyst.

Fig. 5a shows the catalytic performance of VO_x/SiO_2 and V–Sb–O/SiO_2 catalysts in the ODH of propane with O_2 as oxidant from 400 to 650 °C. For both VO_x/SiO_2 and V–Sb–O/SiO_2 catalysts, propene selectivity decreases with propane conversion. This is similar to the catalytic behavior of other vanadium-containing catalysts [5,9,13,16,17]. The V–Sb–O/SiO_2 catalyst is active in the ODH of propane with high propene selectivity but low CO_x selectivity, indicating that the Sb atom isolated VO_x species in antimony–vanadium mixed oxides are highly active and selective in the ODH of propane and the deep oxidation to CO_x can be efficiently depressed over it. Then, V–Sb–O/SiO_2 catalyst results in propene yield comparable to or even higher than that for the ODH of propane catalyzed by V–Mg–O catalysts [3], SBA-15/MCM-41supported vanadia catalysts [5,8] and vanadium-containing mesoporous silica materials [12,13,16] also with O_2 as oxidant. On the contrary, VO_x/SiO_2 catalyst leads to much more CO_x but less propene than V–Sb–O/SiO_2 catalyst due to more aggregated VO_x species over VO_x/SiO_2 catalyst than that over V–Sb–O/SiO_2 catalyst as suggested by UV–Vis DRS and Raman results. At 600 °C, a 65.6% C_3H_6 selectivity with a 40.1% C_3H_8 conversion was obtained. In Fig. 5b, it can be observed that
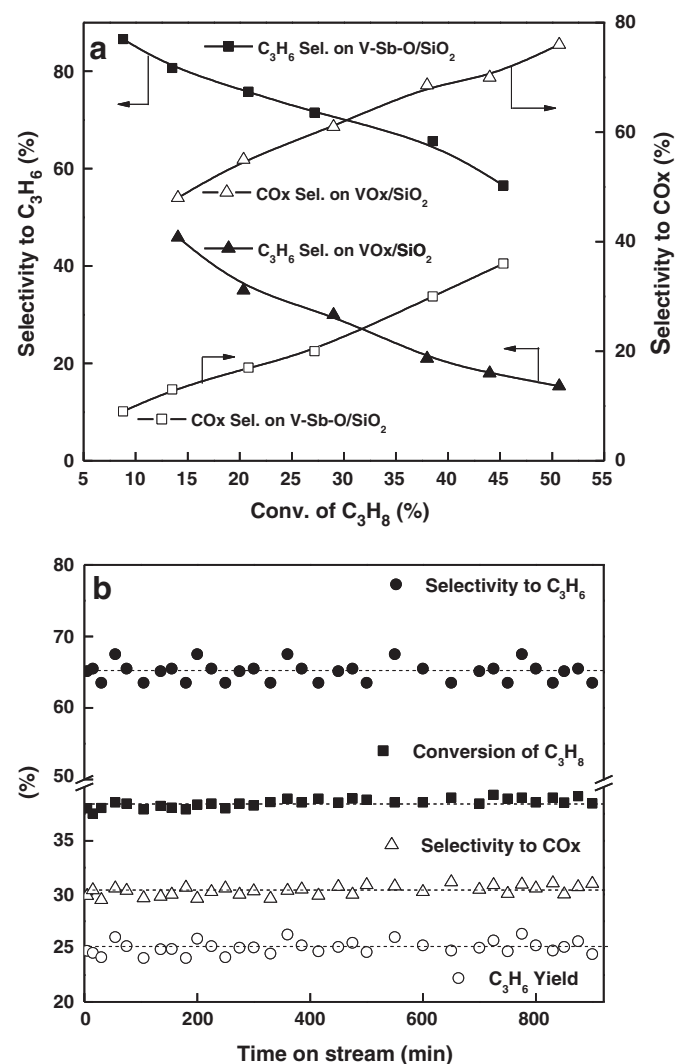

Fig. 4. Raman spectra of SbO_x/SiO_2, VO_x/SiO_2 and V–Sb–O/SiO_2 catalysts. $\lambda_{ex} = 325$ nm.

Fig. 5. Catalytic performance of VO_x/SiO_2 and V–Sb–O/SiO_2 catalysts in the ODH of propane with O_2 as oxidant, a) in the temperature range from 400 to 650 °C, and b) at 600 °C.

a propene yield at 26.3% was achieved over V–Sb–O/SiO$_2$ catalyst at 600 °C and the catalytic behavior was well kept in a 15 h long test. This reflects that the active sites of V–Sb–O/SiO$_2$ catalyst is stable under reaction conditions.

4. Conclusions

This work presents a new route to obtain highly isolated monomeric VOx species in vanadium-containing catalyst. In the $-O-Sb-O-V-O-Sb-$ frameworks of antimony–vanadium mixed oxide of V–Sb–O/SiO$_2$ catalyst, VOx species are isolated by Sb atoms and thus more monomeric VOx species can be obtained. In the ODH of propane with O$_2$ as oxidant, such V–Sb–O/SiO$_2$ catalyst leads to high activity and propene selectivity but depressed production of COx. A propene yield up to 26.3%, which is comparable to or even higher than that for V–Mg–O catalysts, SBA-15/MCM-41supported vanadia catalysts and vanadium-containing mesoporous silica materials, can be achieved.

Acknowledgments

Appendix A. Supplementary data

Supplementary data to this article can be found online at http://dx.doi.org/10.1016/j.catcom.2013.11.014.

References

[1] R.X. Wu, P.F. Xie, Y.H. Cheng, Y.H. Yue, S.Y. Gu, W.M. Yang, C.X. Miao, W.M. Hua, Z. Gao, Catal. Commun. 39 (2013) 20–23.
[2] B. Schimmoeller, J.Y. Jiang, S.E. Pratsinis, A. Baiker, J. Catal. 274 (2010) 64–75.
[3] M. Chaar, D. Patel, M. Kung, H.H. Kung, J. Catal. 109 (1998) 463–467.
[4] T. Blasco, J.M.L. Nieto, Appl. Catal. A 157 (1997) 117–142.
[5] Y.M. Liu, Y. Cao, N. Yi, W.L. Feng, W.L. Dai, S.R. Yan, H.Y. He, K.N. Fan, J. Catal. 224 (2004) 417–428.
[6] S.A. Karakoulia, K.S. Triantafyllidis, G. Tsilomelekis, S. Boghosian, A.A. Lemonidou, J. Catal. 141 (2009) 245–253.
[7] G.L. Dai, Z.H. Li, J. Lu, W.N. Wang, K.N. Fan, J. Phys. Chem. C 116 (2012) 807–817.
[8] B. Solsona, T. Blasco, J.M.L. Nieto, M.L. Peña, F. Rey, A. Vidal-Moya, J. Catal. 203 (2001) 443–452.
[9] E.V. Kondratenko, M. Cherian, M. Baerns, D.S. Su, R. Schlögl, X. Wang, I.E. Wachs, J. Catal. 234 (2005) 131–142.
[10] P. Gruene, T. Wolfram, K. Pelzer, R. Schlögl, Catal. Today 157 (2010) 137–142.
[11] R. Schlögl, Top. Catal. 54 (2011) 627–638.
[12] H. Berndt, A. Martin, A. Brückner, E. Schreier, D. Muller, H. Kosslick, G.U. Wolf, B. Lucke, J. Catal. 191 (2000) 384–400.
[13] Y.M. Liu, S.H. Xie, Y. Cao, H.Y. He, K.N. Fan, J. Phys. Chem. C 114 (2010) 5941–5946.
[14] F. Gao, Y.H. Zhang, H.Q. Wan, Y. Kong, X.C. Wu, L. Dong, B.Q. Li, Y. Chen, Microporous Mesoporous Mater. 110 (2008) 508–516.
[15] M. Piumetti, B. Bonelli, M. Armandi, L. Gaberova, S. Casale, P. Massiani, E. Garrone, Microporous Mesoporous Mater. 133 (2010) 36–44.
[16] Q.H. Zhang, Y. Wang, Y. Ohishi, T. Shishido, K. Tekahira, J. Catal. 202 (2001) 308–318.
[17] F. Ying, J.H. Li, C.J. Huang, W.Z. Weng, H.L. Wan, Catal. Lett. 115 (2007) 137–142.
[18] Z.H. Luan, J. Xu, H.Y. He, J. Klinowski, L. Kevan, J. Phys. Chem. 100 (1996) 19595–19602.
[19] Z.H. Luan, M. Hartmann, D.Y. Zhao, W. Zhou, L. Kevan, Chem. Mater. 11 (1999) 1621–1627.
[20] R.K. Grasselli, Top. Catal. 21 (2002) 79–88.
[21] H.D. Zhang, Z.M. Liu, Z.C. Feng, C. Li, J. Catal. 260 (2008) 295–304.
[22] Y.C. Xie, Y.Q. Tang, Adv. Catal. 37 (1990) 1–47.
[23] H.D. Zhang, K.Q. Sun, Z.C. Feng, P.L. Ying, C. Li, Appl. Catal. A 305 (2006) 110–119.
[24] H.D. Zhang, P.L. Ying, J. Zhang, C.H. Liang, Z.C. Feng, C. Li, Stud. Surf. Sci. Catal. 147 (2004) 547–552.
[25] H. Golinska, P. Decyk, M. Ziolek, J. Kujawa, E. Filipek, Catal. Today 142 (2009) 175–180.
[26] M. Baltes, K. Cassiers, P.v.D. Voort, B.M. Weckhuysen, R.A. Schoonheydt, E.F.J. Bansant, J. Catal. 197 (2001) 160–171.
[27] G. Xiong, V.S. Sullivan, P.C. Stair, G.W. Zajac, S.S. Trail, J.A. Kaduk, J.T. Golab, J.F. Brazdil, J. Catal. 230 (2005) 326–335.
[28] H.D. Zhang, L. Zhang, Z.C. Feng, S.G. Wang, K.Q. Sun, P.L. Ying, C. Li, Chin. J. Catal. 26 (2005) 542–544.
[29] M.A. Bañares, I.E. Wachs, J. Raman Spectrosc. 33 (2002) 359–380.
[30] H.D. Zhang, J. Zhang, K.Q. Sun, Z.C. Feng, P.L. Ying, C. Li, Catal. Lett. 106 (2006) 89–93.
[31] C. Li, J. Catal. 216 (2003) 203–216.